

Modelling of *E. coli* distribution for hazard assessment of bathing waters affected by combined sewer overflows

Luca Locatelli ¹, Beniamino Russo ^{1,2}, Alejandro Acero Oliete ², Juan Carlos Sánchez Catalán ², Eduardo Martínez-Gomariz ³, Montse Martínez ¹.

5 ¹ AQUATEC - Suez Advanced Solutions. Ps. Zona Franca 46-48. 08038, Barcelona. Spain.

² Group of Hydraulic and Environmental Engineering (GIHA), Technical College of La Almunia (EUPLA), University of Zaragoza, Mayor St. 5, 50100, Spain.

³ Cetaqua, Water Technology Centre, Environment, Society and Economics Department, Cornellà de Llobregat, 08940, Spain

Correspondence to: Luca Locatelli (luca.locatelli@aquatec.es)

10 **Keywords:** modelling, CSO, urban drainage, water quality, *E. coli*, Bathing Water Directive, hazard and risk assessment

Abstract. Combined Sewer Overflows (CSO) affect bathing water quality of receiving water bodies by bacterial pollution. The aim of this study is to assess the health hazard of bathing waters affected by CSOs. This is useful for bathing water managers, for risk assessment purposes and for further impact and economical assessments. Pollutant hazard was evaluated based on two novel indicators proposed in this study: the mean duration of insufficient bathing water quality (1) over a period
15 of time (i.e. several years) and (2) after single CSO/rain events. Particularly, a novel correlation between the duration of sea water pollution and the event rainfall volume was developed. Pollutant hazard was assessed through a state-of-the-art coupled urban drainage and sea water quality model that was developed, calibrated and validated based on local observations. Furthermore, hazard assessment was based on a novel statistical analysis of continuous simulations over a 9 year period using the coupled model. Finally, a validation of the estimated hazard is also shown. The health hazard was evaluated for the case
20 study of Badalona (Spain) even though the methodology presented can be considered generally applicable to other urban areas and related receiving bathing water bodies. The case study presented is part of the EU funded H2020 project BINGO (Bringing Innovation to Ongoing water management—a better future under climate change).

1 Introduction

Bathing water quality is regulated by the Bathing Water Directive (2006/7/EC) (BWD) and the corresponding transposition
25 law within each EU nations. For instance, in Spain it is the Real Decreto REAL DECRETO 1341/2007. The BWD sets the guidelines for the bathing water monitoring and classification, the management and the provision of information to the public. Short term pollution events (having usual durations of less than 72 hours) like the ones caused by Combined Sewer Overflows (CSOs) lead to insufficient bathing water quality and require additional monitoring/sampling of bathing waters. Model simulations can be used to predict the pollutant plume spatial and temporal evolution in bathing water bodies, however such

30 tools are not widespread (Andersen et al. 2013). In case of moderate and heavy rains, CSOs discharge high concentrations and loads of the bacteria *E. coli* (*Escherichia coli*) and intestinal enterococci (coming from waste and stormwater runoff) in the receiving water bodies where concentrations can exceed the bathing water quality standards. If bathing water quality is insufficient, then local authorities should inform end-users, discourage bathing and collect water samples to monitor bacterial pollution. Generally, safe bathing can be re-established after a collected water sample have shown acceptable bathing water
35 quality.

In the field of risk management, and considering a social based risk approach, the risk can be assessed through the combination of the hazard likelihood and the vulnerability of the system referring to the propensity of exposed elements such as human beings, their livelihoods, and assets to suffer adverse effects when impacted by hazard events (BINGO D4.1, 2016). In this framework, risk can be defined as the combination between hazard and vulnerability (including exposure, sensitivity and
40 recovering capacity) according to literature (Turner et al., 2003; Velasco et al., 2018). Donovan et al. (2008) and Viau et al. (2011) evaluated the risk of gastrointestinal disease associated with exposure of people to pathogens like *E. coli* and Enterococci. In the former study, hazard was assessed by statistical analysis of observed bacterial concentrations during 6 days in a year that was considered as representative whereas in the latter one it was estimated by simple assumptions. Andersen et al. (2013) presented a coupled urban drainage and sea water quality model to quantify microbial risk during a swimming
45 competition where lots of gastrointestinal illnesses occurred due to the presence of CSO in sea water. O’Flaherty et al. (2019) evaluated human exposure to antibiotic resistant-*Escherichia coli* through recreational water.

Several water quality models of receiving water bodies were developed to simulate spatial and temporal variations of bacterial concentrations originating from CSOs and other sources. These water quality models also include hydrodynamic models most of the times. Scroccaro et al. (2010) developed a 3D sea water quality model to simulate bacterial concentrations originating
50 from waste water treatment plant discharges. Jalliffier-Verne et al. (2016) and Passerat et al. (2011) developed river water quality models. Liu and Huang (2012) developed a 2D model of an estuary exposed to tides. Sokolova et al. (2013) and Thupaki et al. (2010) presented hydrodynamic 3D models of lakes to simulate *E. coli* based on pollutant discharges estimated from observations at the affluent rivers and/or sewers. Also, coupled urban drainage and water quality models of receiving water bodies were developed to simulate spatial and temporal variations of bacterial concentrations for bathing water quality affected
55 CSOs (Andersen et al., 2013; Marchis et al., 2013).

None of the studies presented above provided a methodology that combined simulated *E. coli* concentration with hazard criteria to evaluate health hazard of bathing waters affected by CSOs that is the main aim of this study. Health hazard was evaluated based on two novel indicators proposed: the mean duration of insufficient bathing water quality (1) over a period of time (i.e. several years) and (2) after single CSO/rain events. Particularly, a novel correlation between the duration of sea water pollution
60 and the event rainfall volume is presented. This is useful for bathing water managers, for risk assessment purposes and for further impact and economical assessments. For example, the presented correlation can be useful to water managers and regulators to predict how long a rainfall event is going to affect the bathing water quality and when could be the optimal time

to collect bathing water samples. Also, to estimate direct and indirect economic impacts of CSOs on coastal economies as was done in the BINGO project. *E. coli* concentration in the receiving water body were simulated by a coupled urban drainage and sea water quality model that was developed, calibrated and validated based on local observations. Health hazard was then quantified through the coupling of simulated *E. coli* concentrations and hazard criteria that were defined based on the BWD specifications. Furthermore, a novel statistical analysis of continuous simulations over a 9 year period using the coupled model is presented. Finally, a validation of the estimated hazard is also shown. The health hazard of bathing waters affected by CSOs was evaluated for the case study of Badalona (Spain).

70 2 Materials and Methods

2.1 The case study

Figure 1 shows the case study area of Badalona (Spain). Badalona, the fourth city of the Catalonia region, is part of the metropolitan area of Barcelona with an extension of 21 km², 215 000 inhabitants and it is highly urbanized. It has approximately 5 km of bathing sandy beaches facing the Mediterranean Sea. Several CSO points discharge combined sewers along the beaches. Generally, rainfall events larger than few mm cause CSOs and during the bathing season bathing is usually forbidden during at least the 24 hours following a CSO events.

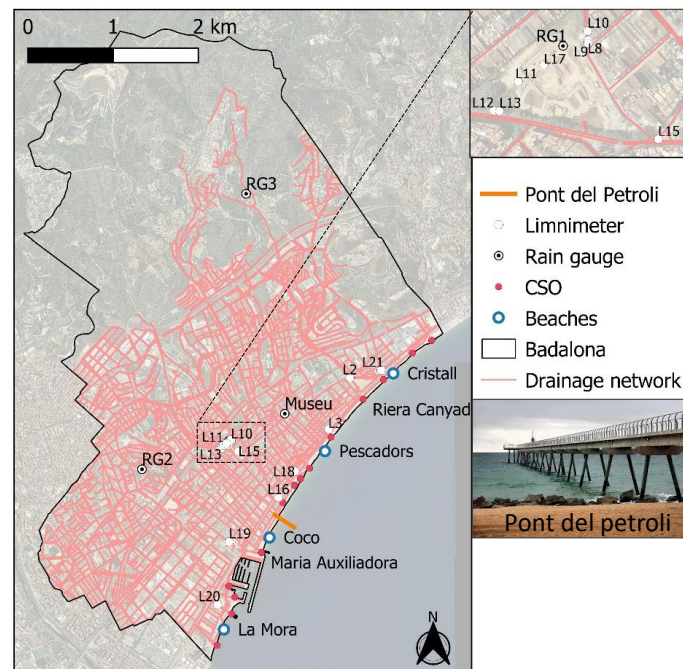
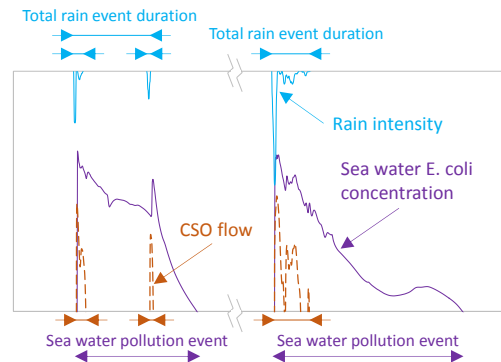


Figure 1. Plan view of Badalona together with the drainage network, the name of some of the beaches, the CSO points, the rain gauges, the limnimeters and the pedestrian bridge Pont del Petroli. Background image from © Google Maps.

80 2.2 Definition of sea water pollution events

Figure 2 shows the definition of a total rain event duration and a sea water pollution event. Two different sea water pollution events are shown for an easier clarification of the definition adopted in this study. The figure shows 3 different rain events, each of them causing CSOs to the sea and 2 different sea water pollution events. The sea water pollution events are defined to occur when bacterial concentrations exceed the selected thresholds. A sea water pollution event can last up to a couple of days and can be generated by different rain/CSO events. Therefore, the definition of a total rain event duration is considered practical for this study considering also the different time scales of the different events involved. A similar definition was introduced in other urban water quality studies analyzing the performance of urban drainage structures such as detention ponds and basins on receiving water bodies (Sharma et al., 2016).



90 **Figure 2. Definition of total rain event duration and sea water pollution event.**

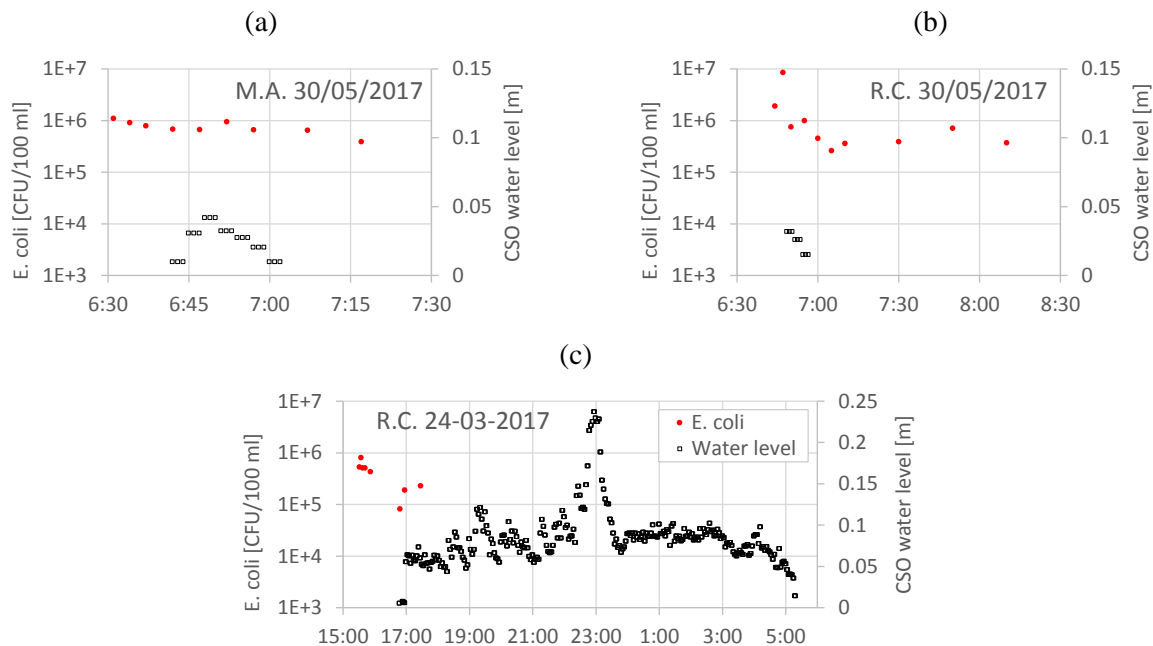
2.3 The data

This section provides an overview of the data collected at the case study. Figure 1 shows the location of the 4 rain gauges and 14 water level sensors that are operating since 2011. These data were relevant for the calibration of the urban drainage model (Section 3.1). The rain gauges RG1, RG2 and RG3 were installed and operational from 2014 providing the time of each tipping of the 0.1 mm buckets 'capacity. The rain gauge of the Museu was installed and operational from 2002 and open access daily rainfall data are available.

Other sensors were also installed in 2015 (as part of the H2020 BINGO project) at the two CSOs points of Maria Auxiliadora and Riera Canyadó (see Figure 1): a radar level and a temperature sensor upstream, and a temperature sensor and a turbidity sensor downstream each of the two weirs. When a CSO occurs, both temperature sensors indicate approximately the same value and the water level sensors are activated, so it is possible to detect the duration of the overflow and the frequency of occurrence of this type of events. These water level data were used for calibration of the simulated CSO hydrographs (obtained by the urban drainage model) at the two observed CSO points (Section 3.1). Also, two automatic 12 bottle samplers were installed to measure CSO turbidity, dissolved oxygen demand, suspended solids and Enterococci and *E. coli* concentrations at the two CSO structures. The measured *E. coli* concentration at CSOs were used for the estimation of CSO concentrations used

105 as inputs for the sea water quality model (Section 3.2). Turbidity, dissolved oxygen demand, suspended solids and Enterococci concentrations were used for other purposes (see H2020 BINGO and LIFE EFFIDRAIN projects) out of the scope of this paper.

Figure 3 shows both the *E. coli* concentration and the CSO water level measured at the two monitored CSO points during the only two events registered: the 30-5-2017 that had 3-4 mm of rain in 3 hours and the 24-3-2017 that had 55-67 mm in 12 hours. 110 During the latter event only data from one (Maria Auxiliadora) of the two monitored CSO structures were available. The water level sensors are located after the weirs and they measured the CSO water levels. Instead, the bottle samplers for *E. coli* concentration measurements were located inside the CSO chamber. Generally, bottle sampling started (the first bottles were filled) before the onset of CSOs. During the CSO event of the 30-5-2017, bottle sampling continued also after the end of the CSO. 115 The automatic bottle sampling frequency was set every 3 minutes for the first bottles up to 30 minutes for the last ones. Figure 3a show 4 *E. coli* measurements during the CSO (CSO is identified by CSO water levels larger than zero) and Figure 3b only 2. These observations are between $5.7 \cdot 10^5$ and $1.0 \cdot 10^6$ CFU/100 ml (Colony Forming Units). Figure 3c shows 3 *E. coli* measurements between $8.2 \cdot 10^4$ and $2.3 \cdot 10^5$ CFU/100 ml during the first 40 minutes of the 12 hours long CSO. Further analysis of such observation was not done due to the sparse data.



120 **Figure 3. *E. coli* concentration and CSO water level measured at the two CSO structures of Riera Canyado (R.C.) and Maria Auxiliadora (M.A.).**

Sea water quality data were measured by the laboratory technicians of the municipality of Badalona during 5 different field campaigns (in the period 2016- 2018) that consisted in taking sea water samples after (sometimes also during) CSO events.

Sea water samples were manually taken at 3 different points (1-close to the shoreline, 2-in the middle of the pedestrian bridge and 3-at the most offshore point) along the approximately 200 m long pedestrian bridge ‘Pont del Petroli’ (Figure 1). The samples were taken once a day (normally between 9AM and 2PM) for the few days following CSO events until bacterial concentrations would recover to small values. The data measured were: *E. coli* and intestinal enterococci concentrations, salinity, turbidity and suspended solids. Sea water quality data are also available from the continuous water quality sampling campaigns that are mandatory in order to classify the water quality at the different bathing locations. For instance, during the last years, more than 400 water samples were collected (and analyzed) at each of the 4 beaches shown in Figure 1 with a sampling frequency of approximately once every couple of weeks. All the water quality indicators were obtained from laboratory analysis of the collected samples. Observed sea water *E. coli* and salinity concentrations were used for calibration and validation of the sea water quality model (Section 3.2) and *E. coli* concentrations also for the validation of the hazard assessment (Section 3.3.1). Sea water turbidity, suspended solids and potential oxygen reduction data were not used in this study.

2.4 The model

A coupled urban drainage and sea water quality model was developed, calibrated and validated based on local observations. The urban drainage model is used to simulate CSO hydrographs at all the CSO points of Badalona. These hydrographs are used as inputs to the sea water quality model to simulate near-shore water quality. The two models are coupled in a sequential way, this means that first the urban drainage and then the sea water quality model are executed. This is acceptable as the physical processes occurring in the sea do not affect CSO hydrographs in Badalona.

2.4.1 The urban drainage model

The urban drainage model aims at simulating CSO hydrographs at the more than 10 CSO structures of Badalona that will then be used as inputs to the sea water quality model. The model simulates rainfall-runoff processes, domestic and industrial sewage water fluxes and hydrodynamics in the drainage network over the whole area of Badalona.

The model was originally developed in MIKE URBAN (www.mikepoweredbydhi.com) for the 2012 Drainage Management Plan (DMP) of Badalona. As part of this study, the model was imported into InfoWorks ICM 8.5 (www.innovyze.com), updated to include the new pipes and one detention tank of approximately 30000 m³ that were constructed during the last years and calibrated and validated with new data. Figure 1 shows the modeled drainage network. Overall, the model includes approximately 368 km of pipes, 11338 manholes, 11954 sub-catchments, 62 weirs, 4 sluice gates and 1 detention tank.

The sewer flows were simulated by the full 1D Saint-Venant equations. Rainfall-runoff processes were simulated for each sub-catchment using a single non-linear reservoir with a routing coefficient that is a function of surface roughness, surface area, terrain slope and catchment width. Initial losses are generally small for both impervious urban areas and green areas (≤ 1 mm) and continuous losses for green areas are simulated using the Horton model. The area of Badalona area was divided into 11954

155 computational sub-catchments of different areas. The sub-catchments were obtained by GIS analysis of the digital terrain model (2 m x 2 m resolution) and have areas in the range of 0.01-1 hectares in the urban areas and 1-100 hectares in the upstream rural areas. Each sub-catchment includes the GIS derived information of impervious area and pervious areas that are used to apply either the impervious or the pervious rainfall-runoff model. Impervious areas have not continuous hydrological losses meaning that all the net rainfall (after initial losses) contributes to stormwater runoff.

160 **Calibration and validation of the urban drainage model**

The urban drainage model was calibrated using a trial and error approach with the objective of minimizing the sum of all the Root Mean Square Errors (RMSE) calculated for each of the observation points. The RMSE was calculated for the duration of each simulated event, usually an hour before the beginning of the rainfall and some hours after the end. Table 1 shows the 3 events selected for calibration and the one for validation. Also the different rainfall intensities, volumes and return periods
 165 evaluated based on local rainfall Intensity-Duration-Frequency curves are shown for each event. It is noted that the selected calibration events have generally high intensities and volumes compared to the majority of the events that can cause CSOs (as mentioned above events larger than few mm usually cause CSOs in Badalona). These events were considered ideal for calibration and validation because of both the significant observed water level variations in the drainage pipes and the overall quality and quantity of the collected rainfall and water level data. Rain data from the rain gauges were applied in the model
 170 using Thiessen Polygons.

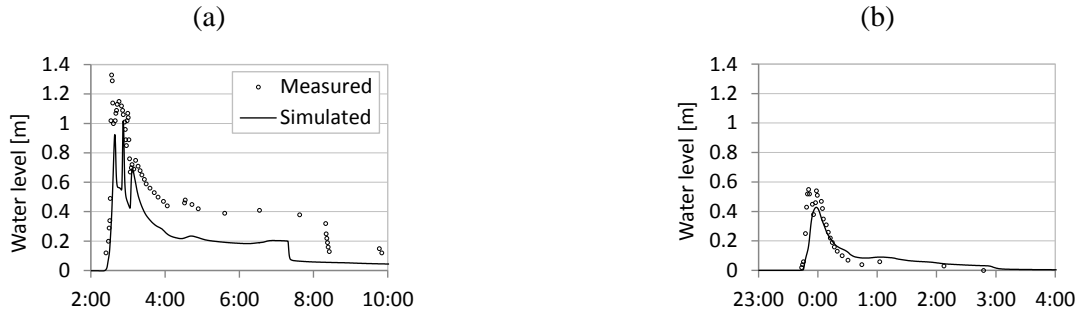
Table 1. Events used for calibration and validation of the urban drainage model

| Date event | P (mm) Cumulative rainfall RG1, RG2, RG3 | I_{20Min} (mm/h) maximum 20 minutes rainfall intensity (T= return period) | I_{5Min} (mm/h) maximum 5 minutes rainfall intensity (T= return period) | Event used for |
|----------------------|--|--|--|-----------------------|
| 22 August 2014 | 18.6, 17.4, 26.0 | 42.6 (T=0.4 y) | 74.4 (T=0.6 y) | Calibration |
| 28-29 July 2014 | 46.5, 36.0, 2.8 | 56.4 (T=0.7 y) | 91.2 (T=0.8 y) | Calibration |
| 03 October 2015 | 33.4, 34.1, 26.0 | 81 (T=2.3 y) | 122.4 (T=1.1 y) | Calibration |
| 13-14 September 2016 | 30.2, 25.2, 20.2 | 64.5 (T=1.1 y) | 142.8 (T=1.3 y) | Validation |

The calibrated Horton parameters were: an initial infiltration capacity of 20 mm/h, a final one of 7 mm/h, a capacity decrease exponent of 0.043 h⁻¹ and a capacity increase exponent 0.108 h⁻¹. The initial loss was not calibrated and it was calculated as
 175 $Value/slope^{0.5}$, where *Value* was set to 0.000071 and 0.00028 m for impervious and pervious surfaces respectively and slope was the average slope of the sub-catchment calculated with GIS. The calibrated Manning's roughness coefficient of surface impervious areas was set to 0.013 and the one of pipes was set to 0.012. The calibrated Manning's roughness coefficients are

in the lowest parts of the ranges proposed in similar urban drainage studies (Fraga et al., 2017; Locatelli et al., 2017; Russo et al., 2015) and more general hydrologic studies (Dingman, 2015; Henriksen et al., 2003).

180 Figure 4 shows two examples of simulated and observed water levels at two different locations during two different rain events. All the other graphs can be found in (BINGO D3.3, 2019). Table 2 shows the computed RMSE and Absolute Maximum Error (AME) (Bennett et al., 2013) for the calibration and validation events. The magnitude of the errors are similar to the ones reported in other urban drainage models (Russo et al., 2015). Overall, the model simulates the observed water levels in the sewer network in an acceptable way.



185 **Figure 4. Example of simulated and measured water levels in the sewer pipes at the location BA15 during the rain event of the 03-10-2015 (a) and at BA2 the 14-09-2016 (b).**

Table 2. Root Mean Square Error (RMSE) and Absolute Maximum Error (AME) for the calibration and validation events.

| | Calibration | | | | | | Validation | |
|--------------------|----------------|---------|--------------|---------|----------------|---------|-------------------|---------|
| | 22 August 2014 | | 28 July 2014 | | 3 October 2015 | | 14 September 2016 | |
| Water level sensor | RMSE [m] | AME [m] | RMSE [m] | AME [m] | RMSE [m] | AME [m] | RMSE [m] | AME [m] |
| L2 | 0.066 | 0.062 | 0.065 | 0.028 | 0.200 | 0.215 | 0.181 | 0.102 |
| L4 | 0.045 | 0.033 | 0.049 | 0.218 | 0.150 | 1.422 | 0.057 | 0.022 |
| L8 | 0.008 | 0.075 | 0.005 | 0.032 | 0.011 | 0.055 | 0.021 | 0.027 |
| L9 | 0.157 | 0.666 | 0.000 | 0.322 | 0.006 | 0.733 | 0.001 | 0.321 |
| L10 | 0.103 | 0.725 | 0.098 | 0.501 | 0.087 | 0.472 | 0.101 | 0.128 |
| L11 | 0.212 | 0.627 | 0.222 | 1.150 | 0.495 | 2.390 | 0.244 | 1.333 |
| L12 | 0.123 | 0.019 | 0.167 | 0.340 | 0.295 | 0.790 | 0.189 | 0.169 |
| L13 | 0.094 | 0.315 | 0.094 | 0.565 | 0.713 | 0.907 | 0.238 | 0.631 |
| L15 | 0.236 | 1.036 | 0.195 | 0.656 | 0.322 | 0.315 | 0.183 | 0.791 |
| L16 | 0.264 | 0.537 | 0.032 | 2.065 | 0.850 | 1.828 | 0.147 | 0.357 |
| L19 | 0.131 | 0.214 | 0.099 | 0.617 | 0.209 | 0.686 | - | - |
| L20 | 0.346 | 0.387 | 0.148 | 0.190 | 0.333 | 0.059 | 0.096 | 0.159 |
| L21 | 0.056 | 0.290 | 0.082 | 0.222 | 0.099 | 0.190 | 0.181 | 0.300 |

190 Finally, after the calibration and validation, a further manual adjustment of the simulated CSO flows at the two monitored CSO structures was performed using measurements of CSO water levels during three different CSO events from 2017 (67 mm the 24/03, 22 mm the 27/04 and 4.2 mm the 30/05) and CSO structure geometry (weir crest level and width) of the two monitored CSO structures. The simulated crest level of these 2 weirs was manually adjusted by few cm so that the simulated CSO water levels would better fit (visual judgment) the observed ones. It was verified that this further model adjustment did

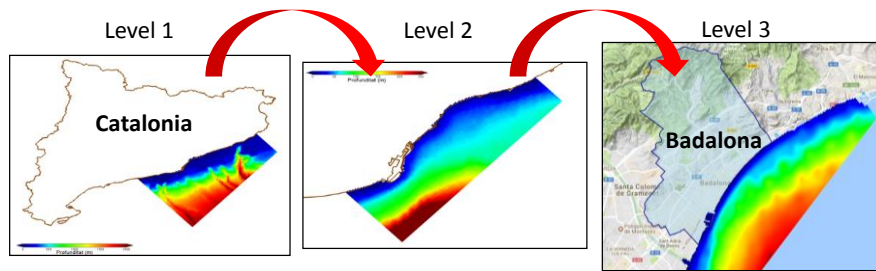
not affect the errors provided in Table 2. The crest level and width values of all the other CSO structures were obtained from
195 the database of the network that came from the DMP of Badalona of 2012.

2.4.2 The sea water quality model

The sea water quality model aims at simulating near shore (within few hundred meters from the shore line) bacterial concentrations in the Badalona sea water during and after CSO events. The water quality model was developed for the area of Barcelona (Gutiérrez et al., 2010) and it is operating since 2007 for real time simulations of bathing water quality of the
200 Barcelona beaches. This model was updated, calibrated and validated for Badalona as part of this study.

The sea water quality model was developed using the software MOHID by MARETEC (Marine and Environmental Technology Research Center) at Instituto Superior Técnico (IST). The model simulates both the hydrodynamics of the sea in the coastal region and the pollutant transport resulting from CSOs.

Simulation of near shore water quality and hydrodynamics during and after CSOs requires spatial discretization scales in the
205 order of tens of meters whereas other coastal hydrodynamic processes can occur at much larger scales. Therefore, 3 model domains are used to simulate hydrodynamic processes from the large regional scale to the local near shore scale of Badalona. Figure 5 shows the three model levels. Level 3 represents city scale processes, $O(10\text{km})$ and is nested into Level 2 that represent sub-regional scale, $O(50\text{km})$, and it is further nested into Level 1, regional scale, $O(200\text{km})$. The 3 levels continuously interact with each other during simulations. Level 1 covers an area of approximately $20,000\text{ km}^2$ with 6500 squared cells of
210 approximately $1 \times 1\text{ km}^2$. At this domain, the hydrodynamic processes of astronomic tides and wind induced waves and currents are simulated in 2D mode (barotropic). Level 2 covers an area of approximately 1000 km^2 with 54000 rectangular cells of sides from 500 m to 200 m (finer cells close to the shore line). Level 3 covers an area of approximately 50 km^2 with 117528 rectangular cells of sides from 200 m to 40 m (finer cells close to the shore line). The vertical discretization of Level 2 and 3 was defined with a Sigma approach with thinner cells close to the sea surface and thicker ones close to the sea bed. The
215 percentages used to define the thickness of each of the 8 vertical layers as a function of the water depth were: 0.458, 0.227, 0.134, 0.079, 0.047, 0.028, 0.017 and 0.01 (the thinnest layer at the sea surface is 1% of the water depth at that location). At Level 2 and Level 3 domains the processes of currents and waves; density, temperature and salinity variations; near shore currents generated by CSOs and river discharges; advection and dispersion of *E. coli* from CSOs are simulated in baroclinic mode with a 3D mesh.



220

Figure 5. The 3 model domains of the sea water quality model. The colors represent the bathymetry (blue=shallow and red=deep). Background image from © Google Maps.

CSOs are simulated in the sea water model as both water discharges and concentration inputs. Water discharge time series at the CSO points are obtained from the urban drainage model and the input concentrations used for CSO discharges were assumed to be fixed (further details are given in the results section).

225

The hydrodynamic model solves the primitive continuity and momentum equations for the surface elevation and 3D velocity field for incompressible flows, in orthogonal horizontal coordinates and generic vertical coordinates, assuming hydrostatic equilibrium and Boussinesq approximations (<http://wiki.mohid.com>). The selected turbulence model was the Smagorinsky model with default values. Wave height and period was computed as function of wind speed, according to ADIOS model formulations (NOAA, 1994).

230

Calibration and validation of the sea water quality model

There different events were used: two for calibration (one in January 2018 and one in September 2016) and one for validation (October 2016). These events were selected because they were the ones with the largest number of sea water *E. coli* and salinity measurements mainly due to both the relatively high observed *E. coli* concentrations and their slow recovering pollutographs.

235

Three events may sound as a limited number for calibration and validation. This was because of the long computational time of the coupled model and because of the data required for bathing water quality models are generally sparse and limited to some events. Similar models in the literature were also based on sparse data and few events for calibration and validation: Marchis et al. (2013) and Passerat et al. (2011) used a single event and Andersen et al. (2013) used 2 events. The computational time of the sea water quality model was in the order of 2 hours per each simulated day using an Intel(R) Core(TM) i5-6200U CPU @ 2.3 GHz processor.

240

Calibration was based on a trial and error approach trying to both optimize the visual fitting between observed and simulated values and to minimize the computed errors. Both *E. coli* concentrations and salinity were used in the calibration process. The 2 calibration parameters (wind drag coefficient and *E. coli* decay rate) were selected after a sensitivity analysis (BINGO D3.3, 2019). A fixed *E. coli* concentration of $1 \cdot 10^6$ CFU/100 ml was used as input for the CSO hydrographs. This is a significant influential parameter and such choice was justified after both literature review and by the available observed data that were shown in Figure 3. Different approaches were presented in the literature: Andersen et al., (2013) simulated CSO dilution using

245

a drainage model with a fixed *E. coli* concentration for waste water based on literature review and assuming clean stormwater runoff. Marchis et al. (2013) used 5 events with river discharge and *E. coli* measurements to calibrate both water quantity and quality from the modelled sub catchment. Jalliffier-Verne et al., (2016) estimated the CSO concentrations based on a fixed discharge per person multiplied by the number of people connected to the sewer network. Passerat et al., (2011) observed *E. coli* concentrations of $1.5 \cdot 10^6$ CFU/100 ml for a CSO where 89% of the discharge were estimated to be from stormwater runoff. McCarthy et al. (2008) analyzed 56 wet rainfall events between 3.2 and 25 mm at 4 different catchments to estimate uncertainty and event mean concentrations of *E. coli*. Wind data for these events were obtained from Puertos del Estado (www.puertos.es). Particularly, a model reproduced observed wind over a selected cell (approximately 10 km long) that covered the area of Badalona and such wind speed was uniformly applied to the sea water quality model.

The calibrated wind drag coefficient was 0.0008. Generally, the higher the coefficient, the higher the sea water velocities and consequent pollutant advection and dispersion. The model MOHID allows either a user defined fixed value that is suggested to be 0.0015 or the use of the function of Large and Pond, (1981) to compute the wind drag coefficient as a function of the wind speed. The calibrated value is within the proposed ranges of Large and Pond, (1981) and Sokolova et al., (2013) used 0.001255. Figure 6 shows the calibrated *E. coli* decay rate expressed as T90, defined as the time at which 90% of the bacterial population is no longer detectable, meaning a one-log reduction of the number of pathogens. T90 could be computed as a function of water temperature, salinity and solar radiation (Canteras et al., 1995; Sokolova et al., 2013). However, such formulations was tested and would produce excessive decay rates for this case study and therefore the decay rate was assumed to have a fixed daily pattern that was calibrated. The calibrated decay rate (Figure 6) shows night T90 values of 4 days (equivalent to $k=0.576 \text{ day}^{-1}=0.024 \text{ h}^{-1}$) and peak daily values of 1.33 days (equivalent to $k=1.73 \text{ day}^{-1}=0.072 \text{ h}^{-1}$). Marchis et al. (2013) and Scroccaro et al. (2010) used fixed day and night T90 values of 1 and 2 days for sea water. For river and lake waters (that are supposed to have slower decay rates compared to salty sea water) Jalliffier-Verne et al. (2016) used fixed day and night decay rates of 0.011 h^{-1} and 0.037 h^{-1} and Passerat et al. (2011) 0.045 h^{-1} . In this case the same fixed decay rates were applied to calibration events during both winter and summer periods even though winter decay rates are likely to be slower due to lower water temperature and solar radiation.

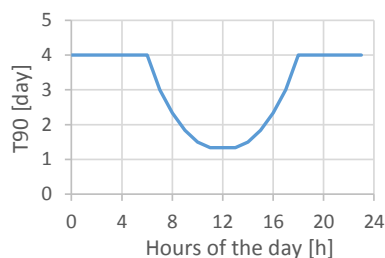


Figure 6. Calibrated *E. coli* decay rate.

Figure 7a, c and e show the simulated versus the observed *E. coli* concentrations for the calibration and validation events at the near-shore sampling point at the Pont del Petroli. Upper and lower bounds of the simulated concentrations are also shown

275 and were obtained by running the model using both 10^7 and 10^5 CFU/100 ml as fixed *E. coli* concentration input at the CSO points (the continuous black line uses 10^6 CFU/100 ml). Despite the sparse data, the model seems to be able to reproduce the observed concentrations with an order of magnitude precision. Figure 7b, d and f show the simulated versus the observed salinity concentrations at the near-shore sampling point at the Pont del Petroli. It is noted that during rainfall events the near shore sea water salinity falls significantly due to the discharge of not salty CSO water into the sea of Badalona. The sea water salinity recovers to typical sea water concentrations (37.5-38 ‰) within some hours, faster than the time it takes for *E. coli* to recover below 500 CFU/100 ml. Due to the daily resolution of observed data, observed peaks of *E. coli* and salinity were poorly detected.

280

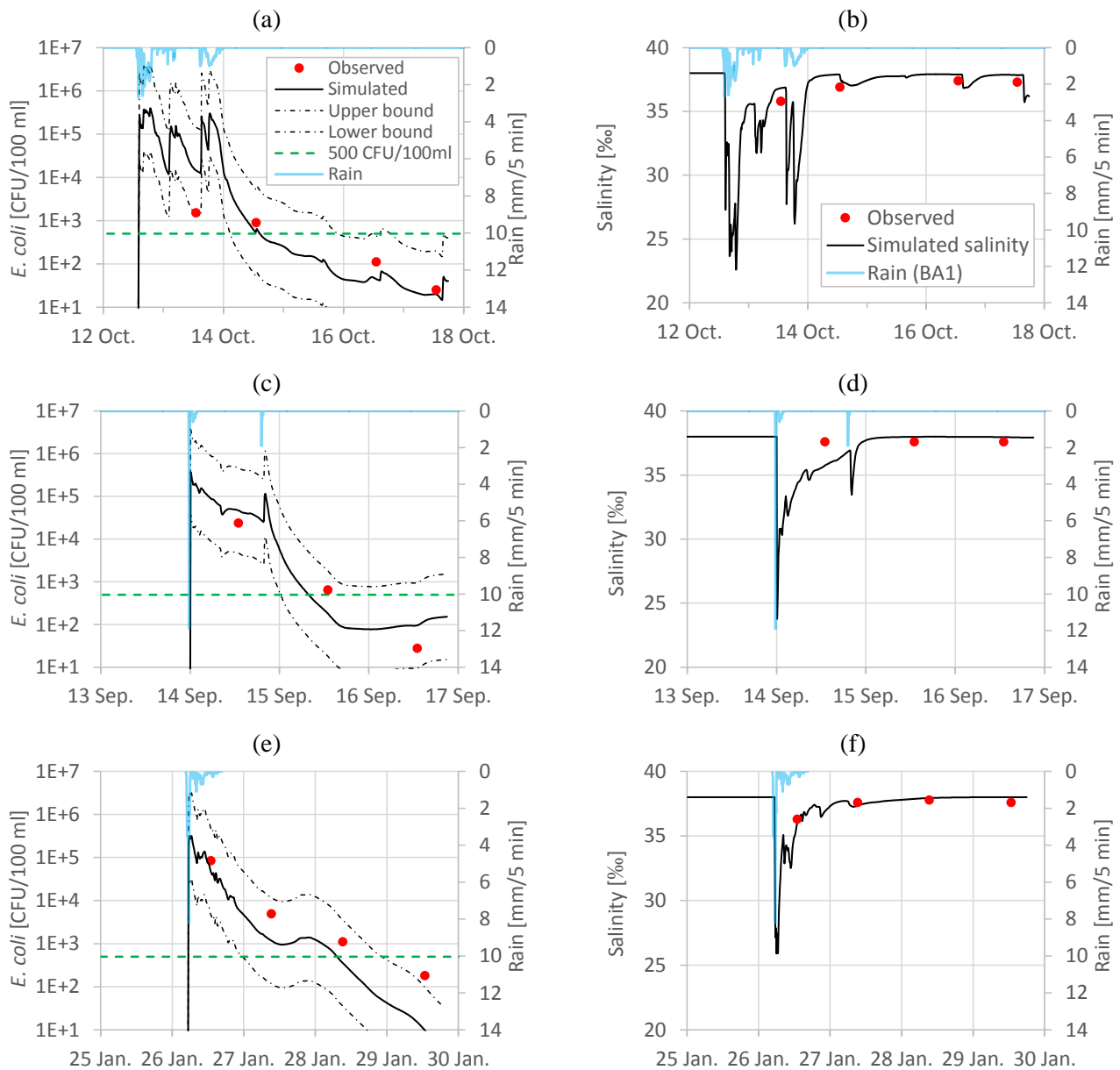


Figure 7. Near-shore simulated and observed *E. coli* concentrations (a, c and e) and salinity (b, d and f) for the calibration and validation events.

285

Figure 8 shows scatter plots of simulated and observed *E. coli* concentrations (a) and salinity (b). The simulated *E. coli* concentrations are shown to reproduce the observed ones with an order of magnitude accuracy. Order of magnitude *E. coli* concentration accuracy is considered acceptable (Pongmala et al., 2015), particularly when simulating concentrations in receiving water bodies where models can be assessed at the order of magnitude level (Dorner et al., 2006). Salinity also seem to somehow follow the 1:1 line of simulated versus observed concentrations even though the majority of the observed values

290

fall within 36 and 38 ‰ that might be a small range compared to the simulated values that can get down to less than 25 ‰ due to CSOs (Figure 7b, d and f).

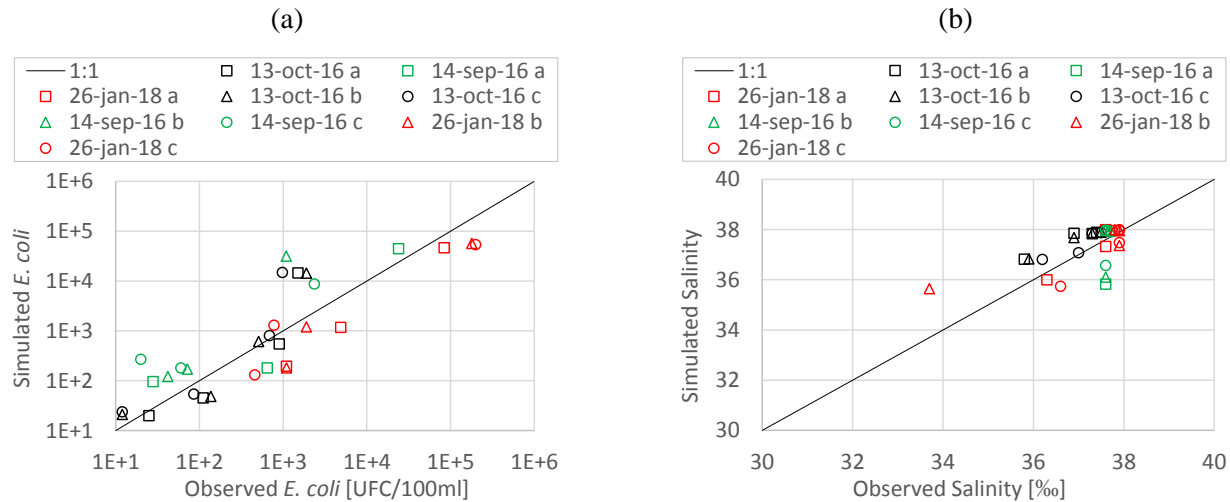


Figure 8. Scatter plots of simulated and observed *E. coli* concentrations (a) and salinity (b).

Table 3 shows the model performance parameters for the calibration and validation events. Log (base 10) Transformed Root Mean Square Error (LTRMSE), Mean Square Log (with base 10) Error (MSLE) and Pearson Product moment correlation (PPMC) were used for *E. coli* and Root Mean Square Error (RMSE) for salinity (Bennett et al., 2013; Hauduc et al., 2015). Few studies reported model performance errors for *E. coli* concentrations in receiving water bodies. Thupaki et al. (2010) obtained a LTRMSE of 0.41 and Liu et al. (2006) in the range of 0.705-0.835. Chen et al. (2019) obtained RMSE error values for salinity simulations of an estuary in the range of 0.13-3.01.

Table 3. Model performance parameters.

| | | | |
|-----------------------------------|------------------------------|---------------------------------|------|
| Calibration and validation events | <i>E. coli</i> concentration | MSLE | 0.44 |
| | | LTRMSE | 0.66 |
| | | Pearson correlation coefficient | 0.83 |
| | Salinity concentration | RMSE [‰] | 0.73 |

It is noted that the 3 events used for calibration and validation of the sea water quality model are from September, October and January. It could be relevant to look at more events during the bathing season that is the focus period of the hazard assessment.

2.5 Hazard assessment

Table 4 shows the hazard criteria applied. The selected approach is similar to the one proposed in the BWD and the REAL DECRETO 1341/2007 to classify bathing water quality. High hazard (*E. coli* > 500 CFU/100 ml) is here considered as insufficient bathing water quality.

Hazard is quantified based on two novel indicators proposed that were computed for every beach of Badalona by continuously simulating 9 consecutive bathing seasons (here assumed to be from 1st of June to 1st of September) from 2006 to 2014 using the coupled (urban drainage – sea water quality) model:

- the duration of insufficient bathing water quality over a bathing season.
- the duration of insufficient bathing water quality after rain/CSO events. Particularly, the duration of insufficient bathing water quality is presented as a function of the event rainfall volume.

Both wind data and rainfall data between 2006 and 2014 (9 years) were obtained from the station of Fabra (approximately 10 km away from Badalona) located in the neighbor city of Barcelona. Data from Fabra were used as 9 years of continuous high resolution data were not available from Badalona.

Hazard maps were also analyzed. However, together with the project stakeholders, they were not considered to be an interesting output because of the time and spatial variation of hazard during each different pollution event. Finally, a validation of the hazard assessment is shown for the duration of insufficient bathing water quality after rain/CSO events.

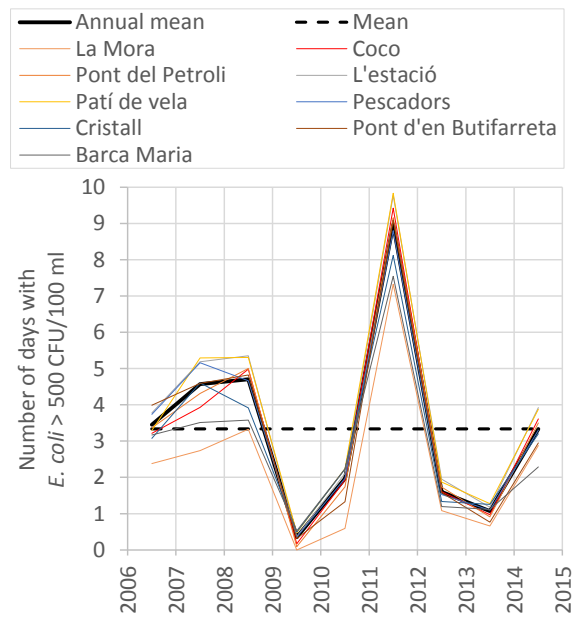
Table 4. Hazard criteria based on *E. coli* concentration in sea water

| Hazard criteria | <i>E. coli</i> concentration [CFU/ 100 ml] |
|-----------------|--|
| Low | <250 |
| Medium | 250<x<500 |
| High | >500 |

3 Results

3.1 Hazard assessment

Figure 9 shows the average number of days with high hazard at the different beaches of Badalona and for the 9 consecutive bathing seasons from 2006 to 2014. The annual average number of days (the thick black line) with high hazard is in between 0 and 9 days per bathing season every year with an overall mean of 3-4 days per bathing season (the black dashed line). The results show a high variability that is highly related to the number and volume of rainfall events occurring during the different bathing seasons. The variability among the different beaches during the same bathing season is smaller compared to the variability due to different years.



330 **Figure 9. Simulated number of days per bathing season with high hazard (*E. coli* concentrations > 500 CFU/100 ml) at all the different beaches of Badalona.**

Successively, the duration of every single sea water pollution event (defined in Figure 2) was correlated to the total rainfall volume that fell during the same sea water pollution event (the total rain event duration of Figure 2) and the results are shown in Figure 10a. Figure 10a shows an example of the results from the Coco beach, even though all beaches were analyzed and all the graphs can be found in the delivery D4.4 of the BINDO project. Overall, the results show that the higher the rainfall volume, the longer the time period the beach is exposed to *E. coli* concentrations above threshold; however, above 15-25 mm of rain volume the increasing tendency seems to vanish; also, only rainfalls above few mm can cause sea water *E. coli* concentrations > 500 CFU/100 ml. The large spreading of the correlation plots is mainly due to the different total rain event duration and the magnitude of marine currents. Overall, longer rain events produce longer CSOs and therefore longer sea water pollution events. Similarly, stronger winds and rougher sea produce shorter sea water pollution events.

Figure 10b is a rearrangement of Figure 10a and shows the probability distribution of sea water pollution events as a function of the rainfall volume. The discretization of the rainfall volume (x-axes) into 4 ranges was chosen in order to obtain both a reasonable number of events simulated in each range and volume ranges that are considered reasonable for local applications. This statistical approach that considered the total rainfall volume was considered the best one among several attempts of correlation between sea water pollution duration and rain intensities of different duration (30, 60, 120, etc. minutes rainfall). Figure 10b provides one of the two main indicators proposed in this study: the duration of high hazard (insufficient bathing water quality) as a function of the event rainfall volume. For instance an event of 12 mm rainfall (that would fall in the bin of $8 \leq x < 16$ mm of Figure 10b) is estimated to produce a median of 0.5 days of high hazard at the Coco beach. The percentiles

provided with the whisker boxes include an estimation of inter event uncertainty obtained by continuous simulations using the
350 deterministic coupled model. Other uncertainties like the ones associated to selected and calibrated parameters were not
addressed.

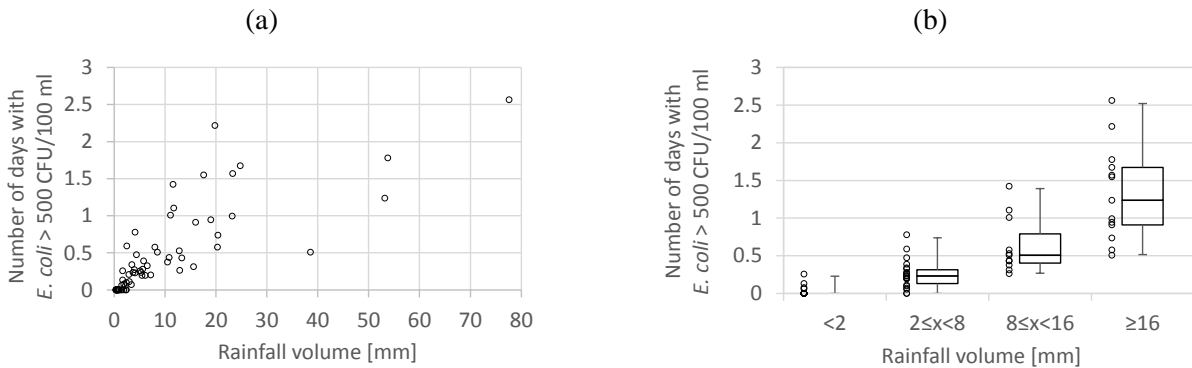
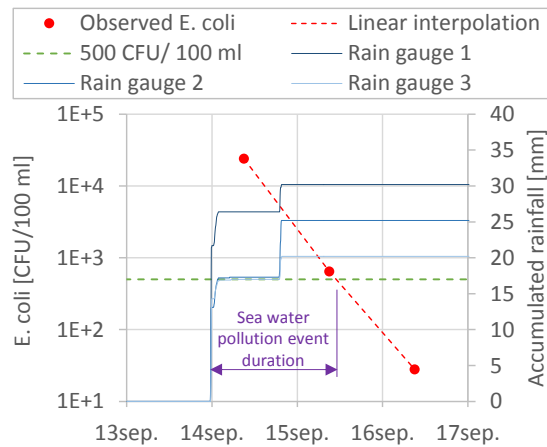


Figure 10. (a) Correlation between the simulated number of days with sea water *E. coli* concentrations above 500 CFU/100 ml at the Coco beach and the rainfall volume. (b) The rainfall volume is categorized into 4 different ranges. The whisker boxes show 1st, 25th, 50th, 75th and 99th percentiles.

355 3.1.1 Validation of the hazard assessment

A validation was performed only for the indicator of high hazard as a function of the event rainfall. The validation of the mean duration of high hazard per bathing season was not done due to lack of observed data. The number of days when bathing was forbidden during bathing seasons are available. However, these data cannot be compared with the simulated high hazard because bathing forbidden days are dependent on local protocols that for instance in the case of Badalona allow the
360 reestablishment of bathing permissions only after positive bathing water quality measurements that usually take more than 24 hours to be obtained.

Figure 11 shows an example of how the duration of a sea water pollution event was graphically obtained based on rainfall data and observed *E. coli* concentrations. The sea water pollution event is assumed to start when the accumulated rainfall exceeds 1 mm. An analysis of the simulation results showed that a sea water pollution event can start up to an hour later compared to
365 the proposed beginning point. This depends on how far from the CSO is the control point and also on the CSO events can start with a delay compared to the rainfall. The sea water pollution event is supposed to end when the simple linear interpolation (the red dashed line of Figure 11) between measured concentrations crosses the selected threshold of 500 CFU/100 ml. The total rainfall associated to the sea water pollution event is the average total volume (from the available rain gauges) that fell during the pollution event.



370

Figure 11. Example of how the duration of a sea water pollution event was graphically obtained.

Figure 12a shows the comparison between the simulated and observed high hazard duration. 8 events were used for the comparison. Overall, the majority of the observed durations fall within the simulated 1st and 99th percentiles. However, there are some outliers. The 2 outliers at the Mora beach are likely because this beach is close to the mouth of the Besos River that might not be properly represented in the model. Also, there are several model uncertainties that were not simulated (for example, input parameters and calibration uncertainties). Further, it seems that the observed values are in the higher range of the simulated percentiles, this can be because all the CSO events that caused little sea water pollution could not be measured by the available sampling resolutions (approximately a sample per day). Overall, this can be considered as a preliminary visual validation.

375 For risk assessment purposes (as part of the BINGO project), together with the project stakeholders, it was decided to adjust/calibrate the proposed percentiles duration in order to obtain a deterministic maximum durations of high hazard that is shown in Figure 12b. For this purpose, several steps were applied: the observed sea water pollution duration derived from intestinal enterococci observations was compared to the simulated *E. coli* percentiles durations of Figure 12a; all the beaches were merged into a unique representative value of pollution duration obtained from the worst 99.9 percentile among all the beaches; finally, a further safety factor of 5% was applied so that all the outliers would be accommodated within the newly developed bars representing a practical deterministic value of maximum sea water pollution duration as a function of 4 different rainfall ranges.

385

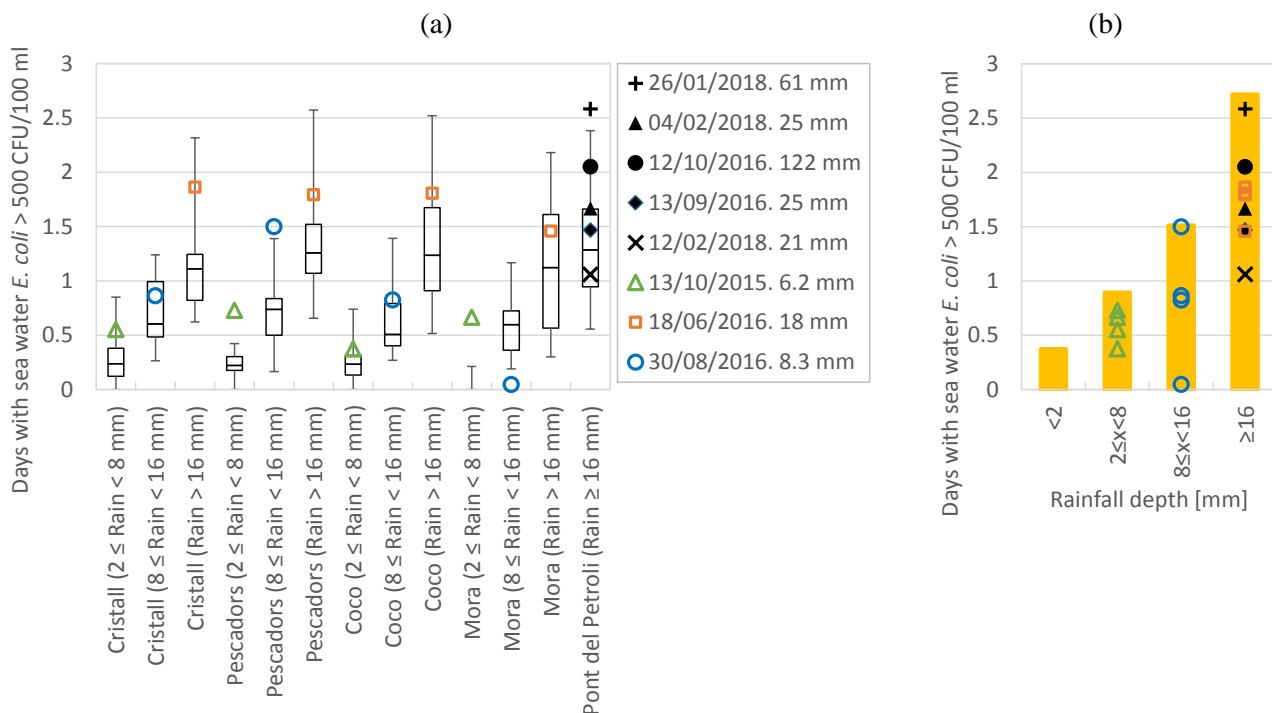


Figure 12. (a) Comparison between the estimated and the observed duration of high hazard (sea water *E. coli* > 500 CFU/100 ml). The whisker boxes show 1st, 25th, 50th, 75th and 99th percentiles of the duration of sea water pollution. (b) Maximum sea water pollution duration (orange bars) as a function of 4 different rainfall ranges.

390

4 Conclusions

This study quantified the health hazard of bathing waters affected by CSOs based on two novel indicators: the mean duration of insufficient bathing water quality (1) per bathing season and (2) after single CSO/rain events. Overall, a great uncertainty is associated to the evaluated pollutant hazard, mainly due to the variability of water quality variables, rainfall patterns and sea water currents. A novel correlation between the duration of sea water pollution and the event rainfall volume was presented. Also, a state-of-the-art coupled urban drainage and sea water quality model was developed, calibrated and validated based on local observations. Furthermore, hazard assessment was based on a statistical analysis of the continuous simulations simulation results of 9 consecutive bathing seasons using the coupled model. Finally, a validation of the estimated hazard was also shown. The pollutant hazard of bathing waters affected by CSOs was assessed for the case study of Badalona (Spain) even though the methodology presented can be considered generally applicable to other urban areas and related receiving bathing water bodies. The results of this study were useful as inputs for risk assessment and to analyze direct, indirect, tangible and intangible impacts related to CSO and consequent pollution of sea water. Also, the correlation presented to predict the duration of insufficient bathing water quality as function of the observed rainfall volume can be useful to bathing water managers.

395

400

Acknowledgments

405 This study was conducted as part of the BINGO European H2020 project (Grant Agreement No.641739, <http://www.projectbingo.eu/>). The authors thank the Municipality of Badalona and particularly Antonio Gerez Angulo, Maria Luisa Forcadell Berenguer, Gregori Muñoz-Ramos Trayter and Josep Anton Montes Carretero for their valuable contributions. Also, thanks to the LIFE EFFIDRAIN project (LIFE14 ENV/ES/000860. <http://www.life-effidrain.eu/>) for shearing data.

Competing interests

410 The authors declare that they have no conflict of interest.

Code/Data availability

Model files and data are not provided.

Author contribution

Beniamino Russo, Montse Martinez and Luca Locatelli coordinated the research project. Alejandro Acero Oliete and, Juan
415 Carlos Sánchez Catalán managed the data collection. Luca Locatelli, Beniamino Russo and Eduardo Martinez-Gomariz developed the conceptual model and Luca Locatelli set-up the model, did the code and performed the simulations. Luca Locatelli prepared the manuscript with the contributions of all co-authors.

References

- Andersen, S. T., Erichsen, A. C., Mark, O. and Albrechtsen, H. J.: Effects of a 20 year rain event: A quantitative microbial risk assessment
420 of a case of contaminated bathing water in Copenhagen, Denmark, *J. Water Health*, 11(4), 636–646, doi:10.2166/wh.2013.210, 2013.
- Bennett, N. D., Croke, B. F. W., Guariso, G., Guillaume, J. H. A., Hamilton, S. H., Jakeman, A. J., Marsili-Libelli, S., Newham, L. T. H., Norton, J. P., Perrin, C., Pierce, S. A., Robson, B., Seppelt, R., Voinov, A. A., Fath, B. D. and Andreassian, V.: Characterising performance of environmental models, *Environ. Model. Softw.*, 40, 1–20, doi:10.1016/j.envsoft.2012.09.011, 2013.
- BINGO D3.3: Calibrated water resources models for past conditions, H2020 BINGO. Bringing Innov. to onGOing water Manag. – a better
425 Futur. under Clim. Chang. Grant Agreem. n° 641739 [online] Available from: http://www.projectbingo.eu/downloads/BINGO_Deliverable3.3_submitted.pdf, 2019.
- BINGO D4.1: Context for risk assessment at the six research sites, including criteria to be used in risk assessment, H2020 BINGO. Bringing
Innov. to onGOing water Manag. – a better Futur. under Clim. Chang. Grant Agreem. n° 641739 [online] Available from:
http://www.projectbingo.eu/downloads/BINGO_Deliverable4.1.pdf, 2016.
- 430 Canteras, J. C., Juanes, J. A., Pérez, L. and Koev, K. N.: Modelling the coliforms inactivation rates in the Cantabrian Sea (Bay of Biscay) from in situ and laboratory determinations of t90, *Water Sci. Technol.*, 32(2), 37–44, doi:10.1016/0273-1223(95)00567-7, 1995.
- Chen, J., Liu, Y., Gitau, M. W., Engel, B. A., Flanagan, D. C. and Harbor, J. M.: Evaluation of the effectiveness of green infrastructure on hydrology and water quality in a combined sewer overflow community, *Sci. Total Environ.*, 665, 69–79, doi:10.1016/j.scitotenv.2019.01.416, 2019.
- 435 Dingman, S. L.: *Physical Hydrology: Third Edition*, Waveland Press. [online] Available from: <https://books.google.es/books?id=rUUaBgAAQBAJ>, 2015.

- Donovan, E., Unice, K., Roberts, J. D., Harris, M. and Finley, B.: Risk of gastrointestinal disease associated with exposure to pathogens in the water of the Lower Passaic River, *Appl. Environ. Microbiol.*, 74(4), 994–1003, doi:10.1128/AEM.00601-07, 2008.
- 440 Dorner, S. M., Anderson, W. B., Slawson, R. M., Kouwen, N. and Huck, P. M.: Hydrologic modeling of pathogen fate and transport, *Environ. Sci. Technol.*, 40(15), 4746–4753, doi:10.1021/es060426z, 2006.
- Fraga, I., Cea, L. and Puertas, J.: Validation of a 1D-2D dual drainage model under unsteady part-full and surcharged sewer conditions, *Urban Water J.*, 14(1), 74–84, doi:10.1080/1573062X.2015.1057180, 2017.
- Gutiérrez, E., Malgrat, P., Suñer, D. and Otheguy, P.: Real Time Management of Bathing Water Quality in Barcelona, *Conf. Pap. NOVATECH.*, 1–10, 2010.
- 445 Hauduc, H., Neumann, M. B., Muschalla, D., Gämmerl, V., Gillot, S. and Vanrolleghem, P. A.: Efficiency criteria for environmental model quality assessment: A review and its application to wastewater treatment, *Environ. Model. Softw.*, 68(3), 196–204, doi:10.1016/j.envsoft.2015.02.004, 2015.
- Henriksen, H. J., Troldborg, L., Nyegaard, P., Sonnenborg, T. O., Refsgaard, J. C. and Madsen, B.: Methodology for construction, calibration and validation of a national hydrological model for Denmark, *J. Hydrol.*, 280(1–4), 52–71, doi:10.1016/S0022-1694(03)00186-0, 2003.
- 450 Jalliffier-Verne, I., Heniche, M., Madoux-Humery, A. S., Galarneau, M., Servais, P., Prévost, M. and Dorner, S.: Cumulative effects of fecal contamination from combined sewer overflows: Management for source water protection, *J. Environ. Manage.*, 174, 62–70, doi:10.1016/j.jenvman.2016.03.002, 2016.
- Large, W. G. and Pond, S.: Open Ocean Momentum Flux Measurements in Moderate to Strong Winds, *J. Phys. Oceanogr.*, 11(3), 324–336, doi:10.1175/1520-0485(1981)011<0324:OOMFMI>2.0.CO;2, 1981.
- 455 Liu, L., Phanikumar, M. S., Molloy, S. L., Whitman, R. L., Shively, D. A., Nevers, M. B., Schwab, D. J. and Rose, J. B.: Modeling the transport and inactivation of *E. coli* and enterococci in the near-shore region of Lake Michigan, *Environ. Sci. Technol.*, 40(16), 5022–5028, doi:10.1021/es060438k, 2006.
- Liu, W. C. and Huang, W. C.: Modeling the transport and distribution of fecal coliform in a tidal estuary, *Sci. Total Environ.*, 431, 1–8, doi:10.1016/j.scitotenv.2012.05.016, 2012.
- 460 Locatelli, L., Mark, O., Mikkelsen, P. S., Arnbjerg-Nielsen, K., Deletic, A., Roldin, M. and Binning, P. J.: Hydrologic impact of urbanization with extensive stormwater infiltration, *J. Hydrol.*, 544, doi:10.1016/j.jhydrol.2016.11.030, 2017.
- Marchis, M. De, Freni, G. and Napoli, E.: Modelling of *E. coli* distribution in coastal areas subjected to combined sewer overflows, *Water Sci. Technol.*, 68(5), 1123–1136, doi:10.2166/wst.2013.353, 2013.
- McCarthy, D. T., Deletic, A., Mitchell, V. G., Fletcher, T. D. and Diaper, C.: Uncertainties in stormwater *E. coli* levels, *Water Res.*, 42(6–7), 1812–1824, doi:10.1016/j.watres.2007.11.009, 2008.
- 465 NOAA: ADIOSTM (Automated Data Inquiry for Oil Spills) user’s manual. Seattle: Hazardous Materials Response and Assessment Division, NOAA., 1994.
- O’Flaherty, E., Solimini, A., Pantanella, F. and Cummins, E.: The potential human exposure to antibiotic resistant-*Escherichia coli* through recreational water, *Sci. Total Environ.*, 650, 786–795, doi:10.1016/j.scitotenv.2018.09.018, 2019.
- 470 Passerat, J., Ouattara, N. K., Mouchel, J. M., Vincent Rocher and Servais, P.: Impact of an intense combined sewer overflow event on the microbiological water quality of the Seine River, *Water Res.*, 45(2), 893–903, doi:10.1016/j.watres.2010.09.024, 2011.
- Pongmala, K., Autixier, L., Madoux-Humery, A. S., Fuamba, M., Galarneau, M., Sauvé, S., Prévost, M. and Dorner, S.: Modelling total suspended solids, *E. coli* and carbamazepine, a tracer of wastewater contamination from combined sewer overflows, *J. Hydrol.*, 531, 830–839, doi:10.1016/j.jhydrol.2015.10.042, 2015.
- 475 Russo, B., Sunyer, D., Velasco, M. and Djordjević, S.: Analysis of extreme flooding events through a calibrated 1D/2D coupled model: the case of Barcelona (Spain), *J. Hydroinformatics*, 17(3), 473, doi:10.2166/hydro.2014.063, 2015.
- Scroccaro, I., Ostoich, M., Umgiesser, G., De Pascalis, F., Colugnati, L., Mattassi, G., Vazzoler, M. and Cuomo, M.: Submarine wastewater discharges: Dispersion modelling in the Northern Adriatic Sea, *Environ. Sci. Pollut. Res.*, 17(4), 844–855, doi:10.1007/s11356-009-0273-7, 2010.
- 480 Sharma, A. K., Vezzano, L., Birch, H., Arnbjerg-Nielsen, K. and Mikkelsen, P. S.: Effect of climate change on stormwater runoff characteristics and treatment efficiencies of stormwater retention ponds: a case study from Denmark using TSS and Cu as indicator pollutants, *Springerplus*, 5(1), doi:10.1186/s40064-016-3103-7, 2016.
- Sokolova, E., Pettersson, T. J. R., Bergstedt, O. and Hermansson, M.: Hydrodynamic modelling of the microbial water quality in a drinking water source as input for risk reduction management, *J. Hydrol.*, 497, 15–23, doi:10.1016/j.jhydrol.2013.05.044, 2013.
- 485 Thupaki, P., Phanikumar, M. S., Beletsky, D., Schwab, D. J., Nevers, M. B. and Whitman, R. L.: Budget analysis of *Escherichia coli* at a Southern Lake Michigan Beach., *Environ. Sci. Technol.*, 44(3), 1010–1016, doi:10.1021/es902232a, 2010.
- Turner, B. L., Kasperson, R. E., Matsone, P. A., McCarthy, J. J., Corell, R. W., Christensen, L., Eckley, N., Kasperson, J. X., Luers, A., Martello, M. L., Polsky, C., Pulsipher, A. and Schiller, A.: A framework for vulnerability analysis in sustainability science, *Proc. Natl. Acad. Sci. U. S. A.*, 100(14), 8074–8079, doi:10.1073/pnas.1231335100, 2003.
- 490 Velasco, M., Russo, B., Cabello, Termes, M., Sunyer, D. and Malgrat, P.: Assessment of the effectiveness of structural and nonstructural measures to cope with global change impacts in Barcelona, *J. Flood Risk Manag.*, 11, S55–S68, doi:10.1111/jfr3.12247, 2018.

Viau, E. J., Lee, D. and Boehm, A. B.: Swimmer risk of gastrointestinal illness from exposure to tropical coastal waters impacted by terrestrial dry-weather runoff, *Environ. Sci. Technol.*, 45(17), 7158–7165, doi:10.1021/es200984b, 2011.